



Research article

Novel electro-spun fabrication of blended polymeric nanofibrous wound closure materials loaded with catechin to improve wound healing potential and microbial inhibition for the care of diabetic wound

Yunting Hu, Li Hu, Li Zhang, Juan Chen, Huiyu Xiao, Bin Yu, Yinzhen Pi*

Department of Endocrinology and Metabolism, Changsha First Hospital, Changsha 410000, China

ARTICLE INFO

Keywords:Antibacterial
Antioxidant
Catechin
Chitosan
Diabetes
Wound healing

ABSTRACT

Diabetic wound infections caused by the multiplication of infectious pathogens and their antibiotic resistance. Wound infection evident by bacterial colonization and other factors, such as the virulence and host immune factors. In this context, we need discover appropriate treatment and effective antibiotics for wound infection control. Considering this, we synthesized catechin-loaded polyvinyl alcohol/Chitosan (PVA/CS) based nanofiber for multifunctional wound healing. The physicochemical and biological properties of fabricated nanofiber, were systematically evaluated by various spectroscopy and microscopy techniques. The CA@PVA/CS nanofiber exhibited a high level of antibacterial and antioxidant effects. The nanofibers showed effective control in gram-positive and negative wound infectious bacterial multiplication at the lowest concentration. Based on the 3-(4,5-dimethylthiazol-2-yl)-2,5-diphenyltetrazolium bromide (MTT) cell viability study CA@PVA/CS nanofiber shows excellent biocompatibility against L929 cells. In wound, scratch assay results revealed that the CA@PVA/CS treated group shows enhanced cell migration and cell proliferation within 48 h. The synthesis of antioxidant, antibacterial, and biocompatible nanofiber exposes their potential for effective wound healing. Current research hypothesized catechin loaded PVA/CS nanofiber could be a multifunctional and low-cost material for diabetic wound care application. Fabricated nanofiber would be improved skin tissue regeneration and public health hygiene.

1. Introduction

Diabetic wounds and chronic skin infections affect millions of peoples worldwide [1]. Treatment of diabetic wounds is the biggest challenge because of skin regeneration and migration of cells towards wound sites due to bacterial infection [2,3]. Incurable diabetic wounds have a great impact on patients and cause pain, depression, anxiety, and longtime hospitalization [4–6]. Another side, open diabetic wounds are infected by microorganisms. The large population of microbes in wound sites causes serious suffering and delays the wound healing process [7–10]. Biomaterials used for wound care systems provide several advantages, such as bio-safety, skin permeability to oxygen, adhesive properties, and infection reduction mechanism. The use of bioactive components and fiber scaffolds has a great interest in wound care [11–13]. Plant-derived components or phytochemicals are currently explored as an effective

* Corresponding author.

E-mail address: Yinzhen_Pi@outlook.com (Y. Pi).<https://doi.org/10.1016/j.heliyon.2024.e26940>

Received 16 May 2023; Received in revised form 20 February 2024; Accepted 21 February 2024

Available online 28 February 2024

2405-8440/© 2024 Published by Elsevier Ltd.

This is an open access article under the CC BY-NC-ND license

[\(http://creativecommons.org/licenses/by-nc-nd/4.0/\)](http://creativecommons.org/licenses/by-nc-nd/4.0/).

resource for nanofiber fabrication to improve anti-inflammatory and wound healing efficiency [14–16]. In particular, catechin is a naturally occurring polyphenol with anti-inflammatory, antioxidant, and anticancer effects [17–19]. The ability to cross the blood-brain barrier (BBB) of catechin molecules has led to increased interest in antioxidant-related benefits for infection control and cell regeneration. Oxidative stress plays a vital role in skin cell proliferation activated by intracellular signaling cascades [20–22]. Some reports have elucidated that catechin has reliable potential in blood glucose reduction modulating the glucose transport chain mechanism. The beneficial potential of catechin and its wound care at different stages of wound sites such as inflammation, proliferation, and tissue regeneration [22–24]. On another hand, chitosan has growing interest in wide spectrum in biomedical research, mainly wound care, drug delivery, antimicrobial, and fat binding agent. Chitosan exhibits highly sophisticated functions in biochemical activity, biocompatibility, biodegradability, and low toxicity [25–29]. It is used to prepare films, fibers, and hydrogels, and most of them are used in biomedical applications [30,31]. Recently, the health care process has an intrinsic reorganization of ineffective antibiotics and wound dressing. A variety of antibiotics and wound dresses are available in the commercial market. The inefficient wound repair processes lead to maladaptive regeneration in skin health [32–34]. And other facts such as the excess amount of degrading enzyme, bacterial infections, and lack of vasculature delay the wound healing process. In this context, effective strategy and materials are required to prepare effective wound dressings [35,36]. Nanomaterial based wound dresses are carrying active molecules with fiber scaffolds for multi functionalities. This type of nanofiber scaffold is the most charming formulation due to its mechanical strength, ease of synthesis, biocompatibility, and effectiveness in medical treatments [37–41]. For instance, nanofibers built from biopolymers and plant compounds encapsulation promotes immediate wound closure and skin cell regeneration. Most advanced wound dressing mainly focused on the control of bacterial infections in wound sites [42–45]. The discovery of a novel wound dress via biopolymer and plant compound-based nanofiber is a powerful choice for diabetic wound healing applications. In addition, flexibility, biocompatibility, and active molecule releasing of the wound dressing to be able to decrease the risk of wound care [46–48]. In this study, we reported that the simple electro-spinning fabrication of catechin loaded PVA/CS nanofiber for antibacterial, and antioxidant properties led to diabetic wound healing application. Due to its natural biocompatibility, cell migration, along with antibacterial properties, CA@PVA/CS nanofiber scaffolds might play an excellent role in diabetic wound care and positive influence on epithelial cell regeneration of the wounds.

2. Materials and methods

2.1. Chemicals

Low molecular weight chitosan powder (MW: 1600 kDa), catechin, MTT, Dulbeccos modified eagle medium, fetal bovine serum, polyvinyl alcohol (MW:85 kDa), glacial acetic acid (90–99 % purity, Muller Hinton broth, agar-agar, nutrient broth and nutrient agar, phosphate buffered saline, 2,2-Diphenyl-1-picrylhydrazyl (DPPH), were purchased from Sigma Aldrich.

2.2. Synthesis of CA@PVA/CS nanofibers

Catechin-loaded PVA/CS nanofiber was synthesized by the electrospinning method. Chitosan and catechin were dissolved in 90 % acetic acid to make a 6 wt % chitosan solution and a 2 wt % catechin solution. Polyvinyl alcohol (PVA) was dissolved in hot (80 °C) deionized water to make a 10 wt % solution. The CS/PVA polymeric blended solution have ratio of 0.6:1. After the blended solutions were prepared, they were electrospun simultaneously. A high voltage power supply unit (TL-Pro, Shenzhen, China) was used to generate a voltage of –2 kV–20 kV for the electrospinning process. The solution was injected at a consistent rate via a glass syringe (5 mL) placed in a holder and pushed by a pump. An adjustable high-voltage supply was used to create an electric field, and solutions were injected from a syringe into a silicone tube connector before passing through a blunt-tipped stainless steel needle (gauge 18, inner diameter 0.84 mm). The holder for the needle was mobile, allowing it to move in front of the mandrel. Exhausting fans have been incorporated in the apparatus for the purpose of evaporating the solvents. The revolving mandrel wrapped in aluminium foil was used to gather the leftover polymer chains that had formed the nanofibrous mats. The speed of the mandrel's rotation might be adjusted. On a computerized display, the operator could change settings like TCD, injection rate, mandrel rotation speed, needle scan location, and electric field. The solutions were electrospun at room temperature using the following parameters: 20 kV voltage, 0.5 mL/h injection rate, 100 mm TCD, and 700 rpm mandrel rotation. For the characterization experiments, the nanofibers collected on aluminium foils were kept at ambient temperature.

2.3. Characterization techniques

The morphology of the prepared CA@PVA/CS nanofiber was examined and images were taken by using field emission scanning electron microscopy (FE-SEM Supra 55VP, USA). The nanofiber diameter was assessed by ImageJ software. The active functional groups of prepared nanofibers were evaluated by using FTIR spectroscopy (ATR-FTIR, Lumos, USA) at the range of 400–4000 cm^{-1} . The absorption spectra of catechin and CA@PVA/CS nanofiber were recorded by using a UV-Vis spectrometer (Agilent, USA) the spectra range is 200–800 nm respectively. The tensile strength of CA@PVA/CS nanofiber was tested by SANTAM universal testing machine (STM-1).

2.4. Mechanical characterizations

2.4.1. Rheology analyses

The Anton Paar (Physica TM) MCR300 rheometer was used to examine the characteristics of PVA/CS and CA@PVA/CS solutions. To measure the viscosity of solutions with different combinations, the rheometer utilized cone and plate geometry with diameters ranging from 1° to 0.05° and conical angles of 1°. Using shear rates ranging from 0.01 s⁻¹–1000 s⁻¹, shear viscosities were measured at 25 °C, while shear stresses were measured in the range of 10⁻³ to 10³.

2.4.2. Tensile strength analyses

Nanofibrous mats made of PVA/CS and CA@PVA/CS were also evaluated in this test. We used a single column universal testing machine (Tinius Olsen H1KS, USA) with a 1 kN load cell to obtain stress-strain curves according to ASTM D882-12. A gauge length of 20 mm was taken to be considered when the specimens were cut into strips measuring 0.5 × 5 cm. After placing the samples in the grips, they were subjected to a strain rate of 10 mm/min until they broke. From the stress-strain curves, the average values of Young's modulus of elasticity (E), ultimate tensile strength (UTS), and elongation at break (εb) were determined for samples of each composition. Data are shown as the average ± standard error.

2.4.3. Water contact angle

By measuring the surface contact angle of the nanofiber with a water drop using the sessile drop method, we can examine the impact of CA incorporation into the PVA/CS nanofibrous samples. With careful consideration, a 2 μL drop of water was applied to the surface of every sample, and images were captured of the interface between the liquid and solid using a Canon high resolution camera. The images were processed using the ImageJ software to obtain the contact angle of the drop with the surface. Each sample had a water droplet placed at least three times, and the average ± standard deviation of the contact angles was reported.

2.4.4. Degree of swelling

The formula for determining the degree of swelling (%) was based on the difference between the dry and swollen samples and measured by using following equation (1);

$$D.S. (\%) = \frac{W_0 - W_s}{W_0} \times 100 \quad (1)$$

W₀ is the weight of the dry sample, and W_s is the weight of the enlarged sample after a period has passed.

2.5. Investigation of encapsulation efficiency (%) and drug loading capacity (%)

The drug loading capacity (%) and encapsulation efficiency (%) were investigated by the procedure followed by previous report with some minor modifications [49]. High performance liquid chromatography (HPLC) with a Thermo Scientific C18 reversed phase column and DMF as the mobile phase at a flow rate of 0.5 mL/min was used to determine the encapsulation efficiency (EE) and drug load capacity (DLC) of the CA loaded PVA/CS nanofibrous material. In order to precipitate the polymer, 20 mg of CA loaded PVA/CS nanofibrous material were dissolved in 5 mL of acetonitrile. After filtering through a 0.22 μm Millipore membrane, the drug concentration was measured using high-performance liquid chromatography. The mass ratio of the encapsulated drug to the amount of drug that was initially added was used to calculate the drug encapsulation efficiency. Drug loading capacity (DLC; equation (2)) and encapsulation efficiency (EE; equation (3)) of celestrol were determined using the following equations,

$$DLC (\%) = \left\{ \frac{\text{drug weight in drug loaded NPs}}{\text{weight of drug - loaded NPs}} \right\} \times 100 \% \quad (2)$$

$$EE (\%) = \left\{ \frac{\text{drug weight in drug loaded NPs}}{\text{Weight of drug in feeding}} \right\} \times 100 \% \quad (3)$$

2.6. Antibacterial activity of CA@PVA/CS nanofiber

The antibacterial efficacy of CA@PVA/CS nanofiber was evaluated by disk diffusion method against wound pathogens *Escherichia coli*, *Pseudomonas aeruginosa*, *Staphylococcus aureus*, and *Staphylococcus epidermis*. The culture media was prepared according to the previous method by Prabhu et al., 2020 [44]. Overnight cultured bacterial strains were evenly swabbed on the agar plates. Different doses of CA@PVA/CS (50, 100, and 150 μg/ml) loaded discs fixed on the agar plates. Ampicillin was considered a positive control for the comparison. plates incubated at 37 °C for 12 h for bacterial growth. After the incubation period, the zone of inhibition was measured by using a zone scale.

2.7. Antioxidant activity of CA@PVA/CS nanofiber

The antioxidant efficacy of the prepared nanofiber was evaluated using DPPH radical-scavenging assay [42]. Briefly, a volume of 2 ml of DMSO dilutions equivalent to volumes of CA@PVA/CS, nanofiber was mixed with 2 ml of 100 μg/ml of DPPH. The reaction

solution was maintained at room temperature under dark conditions for 60 min. Neutralization of DPPH was quantified by UV–vis spectroscopy in the 517 nm range. The free radical scavenging potential of CA@PVA/CS nanofiber was confirmed from absorbance of reaction solution after experiment. The percentage of antioxidant potential of nanofiber is calculated to the following equation (4):

$$\% \text{ of inhibition} = \frac{A_0 - A_1}{A_0} \times 100 \quad (4)$$

Where, A_0 is the absorbance of control and A_1 is absorbance of the treated sample.

2.8. Biocompatibility of CA@PVA/CS nanofiber against L929 cells

The biocompatibility of fabricated CA@PVA/CS nanofiber was examined by using an MTT cell viability assay. The human fibroblast L929 cells were cultured in DMEM medium supplemented with 10 % of FBS and penicillin antibiotic at 37 °C under CO₂ flow. The 20 mg of nanofiber was dissolved by DMSO and different concentrations of nanofiber were treated against L929 cells. All experiment was performed in triplicates on a 96-well plate. The absorbance of treated and control cells was measured by a microplate reader (ChroMate- 4300, USA) at 570 nm. The percentage of biocompatibility was assessed from viable and dead cells using cell counting kit-8. Percentage of cytotoxicity calculated by using following equation (5);

$$CT \% = \frac{\text{Absorbance of control} - \text{Absorbance of treated}}{\text{Absorbance of control}} \times 100 \quad (5)$$

2.9. AO/EtBr dual staining assay for determination of apoptosis

Cytotoxicity and morphological changes of CA@PVA/CS nanofiber treated cells were examined against human fibroblast L929 cells. Then, L929 cells were seeded in DMEM and treated by CA@PVA/CS nanofiber at 100 µg/ml concentration. After 24 h incubation, treated cells were stained with AO/EtBr (10 µg/ml) for 15 min. The excess unreacted cells and debris were washed twice with PBS. Cells were cultured without the addition of nanofiber considered a negative control. The reactive oxygen species (ROS) formation and nuclear damage were detected, and images were captured by a fluorescence microscope. The fluorescence intensity and percentage of dead cells was quantified by using ImageJ 1.44 software.

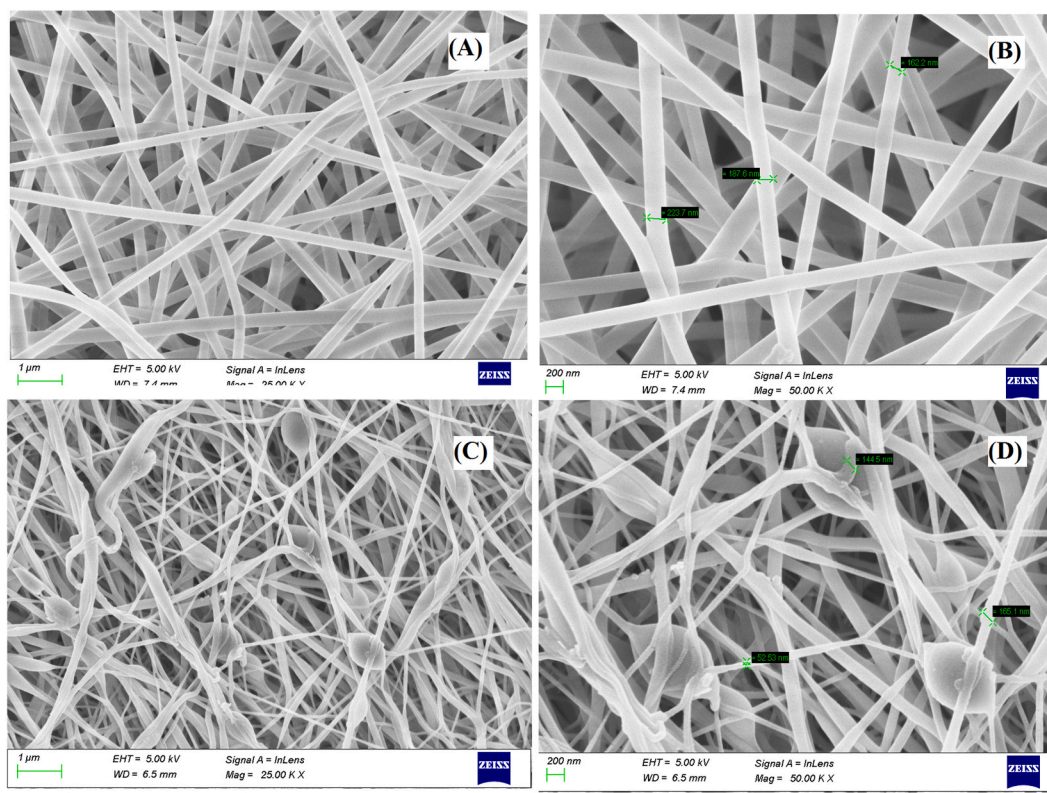


Fig. 1. Field emission scanning electron microscopic images of CA@CS nanofiber (A, B) and CA@PVA/CS nanofiber (C, D) with different magnifications.

2.10. *In vitro* wound scratch assay

The *in vitro* wound healing potential of fabricated CA@PVA/CS nanofiber was examined by using an MTT cell viability assay against fibroblast cells [49]. The skin fibroblast L929 cells were seeded on a twelve-well plate obtained with a monolayer of L929 cells. The IC₅₀ concentration of CA@PVA/CS nanofiber ($78.6 \pm 1.20 \mu\text{g/ml}$) was added into wells containing fibroblast cells. One well treated by commercial anticancer drug cisplatin for comparison of wound healing with nanofiber. Then, a scratch was made by 100 μl micro tip across the middle of wells and washed thrice with phosphate buffer saline to remove detached cells and impurities. A well without nanofiber considers a negative control. Cells were allowed to proliferate under CO₂ flow at 37 °C. The wound closure was examined by Nikon, fluorescence microscope, and images were taken at different time intervals (0, 6, 12, and 24 h). The wound closure area has been calculated using Image J software. The percentage of wound closure and cell migration rate is calculated by the following equation (6);

$$\text{Wound closure \%} = \frac{A_0 - A_t}{A_t} \times 100 \quad (6)$$

A₀ - is the area wound scratch at the time of scratching. A_t - is the area of the wound after the scratches are performed.

2.11. Statistical analysis

All experiments were carried out in triplicates. The IC₅₀ concentration of data were expressed as a mean \pm standard deviation. The characterization techniques and results were analyzed with a one-way ANOVA by Origin 9.0 software. A differential value of *p < 0.05 was considered to be statistically significant.

3. Results

3.1. Morphology and size of CA@PVA/CS nanofiber

The surface morphology of the fabricated nanofiber scaffold was examined by using FE-SEM imaging techniques as shown in Fig. 1. The PVA/CS fibers were obtained at a range of 120–240 nm in diameter. The catechin-loaded CA@PVA/CS was obtained at the range of 50–120 nm diameters in size. It is highly suitable for skin fibroblast cell attachment and cell regeneration. In FE-SEM images of bare PVA/CS nanofibers show smooth and uniform surface morphology in nature (Fig. 1A&B). In this case, catechin-loaded nanofiber showed some irregular morphology in fiber scaffolds, the accumulation of active substances on the surface of nanofibers is generally due to the poor solubility of the active substance in the polymeric matrix (Fig. 1C&D). Moreover, generally, the active substance can form aggregates on the nanofiber surfaces modifying morphological parameters such as the roughness, but do not affect the morphology causing the formation of beads [50,51]. By carefully tailoring the processing parameters, it is possible to obtain uniform fibers even in the absence of beads. Additionally, during specific experiments, the structure of beads could be formed in the fibers as the liquid turns to solid, possibly due to the fact that the electric force rendered the fiber thinner during the fiber-forming process while surface tension decreased the liquid surface area. It indicates that the diameter and beads percent of the obtained fibers were significantly influenced by solution concentration and polymer molecular weight. It was found that as the concentration of the solution increased, the diameters of the smooth fibers obtained increased and the tendency for the observation of beaded fibers reduced. The results demonstrated that the concentration of the solution and the molecular weight of the polymer had distinct impacts on the fiber diameter and the number of beads. In order to produce smaller fibers with bead-free morphologies, the polymer solution needs to be optimized such that the concentration is high enough to cause polymer entanglements but not so high that the viscosity prevents the polymer motion induced by the electric field. The previous research indicates the concentration of the solution and the molecular

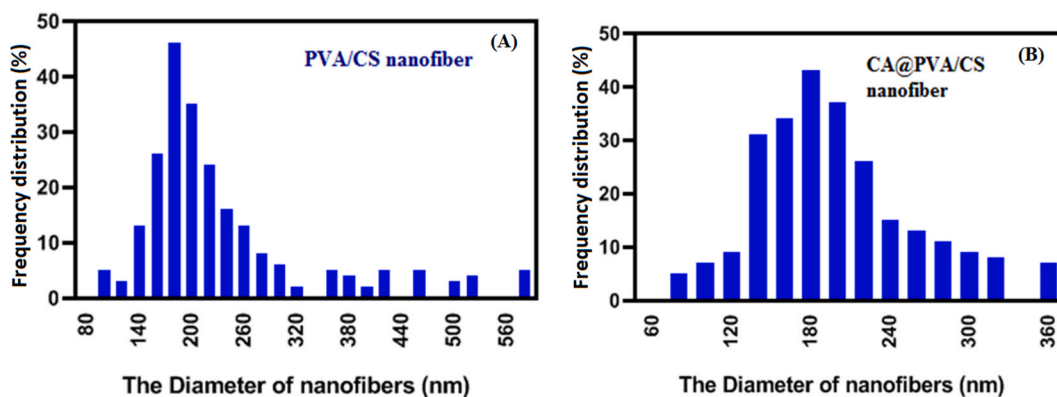


Fig. 2. The nanofibers diameter and stress-strain curve of CA@CS nanofiber (A, C) and CA@PVA/CS nanofiber (B, D).

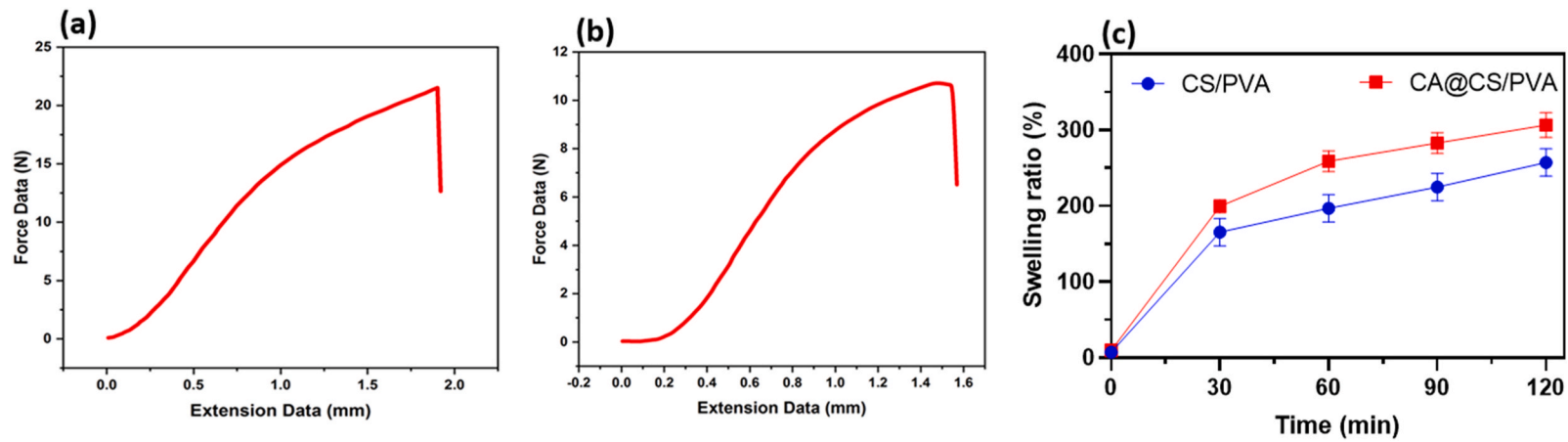


Fig. 3. Mechanical properties of the prepared nanofibrous materials; Stress-strain curve (a & b) and swelling behavior (c) of CA@CS and CA@PVA/CS nanofiber samples.

weight of the polymer had the greatest impact on the fiber diameter and the percentage of beads. Nevertheless, the beads attached to the fibers could serve as a reservoir for drugs or cells; these beads should degrade in a completely different way than the fibers themselves [52–55]. The influence of spinning voltage on the fiber morphology has been investigated by Deitzel et al. They discovered that the formation of defects in the fibers known as beads is strongly correlated with the spinning voltage.

The surface tension increased by the agglomeration of catechin within the fiber scaffold. The average diameter of PVA/CS fiber is 160 ± 15 nm and catechin-loaded CA@PVA/CS nanofiber is 120 ± 10 nm in diameter (Fig. 2 A&B) respectively. The incorporation of catechin with PVA/CS fibers decreases the diameter size of nanofiber scaffolds. The tensile strength of wound care materials plays a prominent role in the healing mechanism. Wound healing agents promote the tensile strength of wound sites. In this study, both CA@CS and CA@PVA/CS nanofiber found to be an ultimate tensile strength at the fracture point shown in Fig. 2. The tensile strength of CA@CS and CA@PVA/CS nanofibers is 21.65 ± 8.3 , and 12.84 ± 5.6 N, respectively (Fig. 3 (a & b)). Table 1 illustrates that the prepared solutions' viscosity increased as CA was incorporated. Intermolecular and intramolecular hydrogen bonding between CS hydroxyl groups on the surface of PVA functional groups is responsible for the increase in solution viscosity, which is caused by the interaction of functional groups of chitosan, PVA, and CA molecules. These findings demonstrated that the CA molecules were effectively enforced into the fibrous polymeric matrix. Table 1 and Fig. 3 (a & b) additionally exhibit the results of the nanofibers' tensile strength and elongation at break. Encapsulation by CA resulted in a substantial reduction in tensile strength for the CA@CS/PVA sample when contrasted with the CS/PVA sample. The tensile strength results demonstrated that chitosan/PVA nanofibers' mechanical strength was slightly reduced after adding CA. As shown in Fig. 3 (b), the stress-strain curves for the tested samples are presented. The tensile strength and elongation at break of the CA@CS/PVA sample are both lower than expected. When CA molecules are incorporated into a polymer matrix, the resulting nanofibrous material typically exhibits this behavior. In Fig. 3 (c), we are able to observe the swelling behavior of PVA/CS nanofibers and CA@CS/PVA nanofibers material. The high surface-to-volume ratio and porous structure of CA@CS/PVA nanofibers enable them to absorb water more rapidly than nanofibrous material. When comparing CS/PVA nanofibers to those with an added CA, a small improvement in water absorption capacity was observed.

The surface properties of tissue engineering scaffolds play an important role in determining the cell/biomaterial interactions. The water contact angle of scaffolds determines the hydrophilicity of the surface which affects the cell growth in cell culture studies. The contact angles of the nanofibers of this study are presented in Table 1. Contact angle for the CS/PVA sample was $54.5 \pm 1.4^\circ$ in accordance with literature data. For the crosslinked nanofibers, the contact angle was slightly increased to $58.7 \pm 3.6^\circ$ indicating a more hydrophobic surface. Crosslinking reactions between PVA and chitosan chains with CA molecules increase the hydrophobicity of the nanofibers. Thus, higher hydrophilicity was observed for CA reinforced nanofibers. Chitosan is a well-known fragile biopolymer the CH-group of chitosan enhances flexibility and stress resistance. In this context, PVA is a flexible polymer the combination of chitosan and PVA ultimately increased the elasticity of the nanofiber scaffold. The incorporation of catechin reduced the size of CA@PVA/CS nanofiber, which leads the reduction in fiber elongation.

3.2. Spectroscopic investigations

The loading of catechin within nanofiber was confirmed using UV–vis spectroscopic observation. The characteristic absorbance of bare catechin is 278 nm. And absorbance of CA@PVA/CS nanofiber shows two regions like as 274 nm and 320 nm respectively (Fig. 4A). In this case alone PVA/CS shows a peak at around 260 nm which indicates the chitosan presence in the nanofiber, and there is no peak at the range of catechin. The peak shifting in CA@PVA/CS nanofiber represents the interaction of catechin and chitosan biopolymer. Chitosan has a high affinity for catechins and can bind with a wide variety of chemical compounds. The amino groups in chitosan can attract the negatively charged polyphenols in catechins through electrostatic interactions. Because of its binding capabilities, chitosan has been investigated for its capacity to increase the bioavailability of particular substances. Chitosan may increase the bioavailability of catechins by facilitating their absorption and retention in the body. The interaction between chitosan and catechins might vary depending on a number of parameters, including the concentration and ratio of the two chemicals, as well as the origin and structure of the chitosan. Further investigation is required in order to fully understand the extent of their interaction and their potential advantages. The characteristic functional groups or specific chemical bonding of CA@PVA/CS nanofiber were examined by FTIR spectroscopic observation as shown in Fig. 4B. A sharp peak at around 1034 cm^{-1} attributes C–O–C stretching vibration. The small peaks around 1144 and 1163 cm^{-1} correspond to the C–O stretching vibrations. The broad band around $3120\text{--}3372 \text{ cm}^{-1}$ wavelength indicates the deformation hydroxyl group from the chitosan and catechin molecules. The peak around 564 cm^{-1} and 2865 cm^{-1} , confirmed the C–N bending and C–H stretching vibrations of chitosan. When PVA polymer and chitosan are combined, they may yield composited material. A novel material with desirable characteristics, such as high mechanical strength, high flexibility, and

Table 1

The analysis parameters of Average diameter (nm), viscosity of the solution, Tensile strength, elongation at break (%) and contact angle ($^\circ$).

Sample	CS/PVA	CA@CS/PVA
Average Diameter (nm)	160 ± 15	120 ± 10
Viscosity of the solution	205 ± 10	196 ± 8
Tensile strength	21.65 ± 23	12.84 ± 3.6
Elongation at Break (%)	15.4 ± 1.3	9.3 ± 0.5
Contact Angle ($^\circ$)	54.5 ± 1.4	58.7 ± 3.6

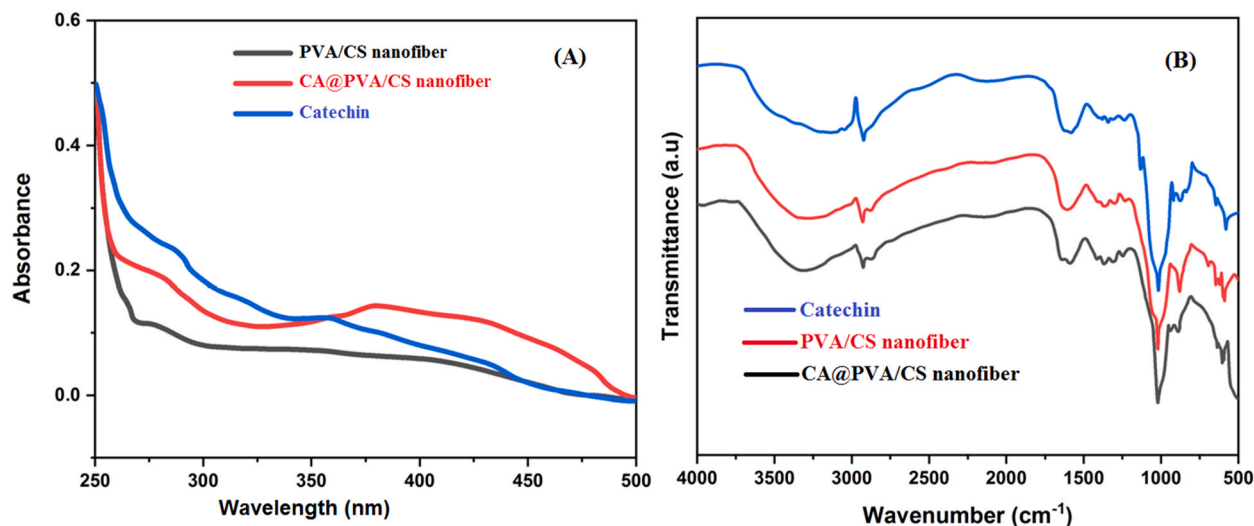


Fig. 4. (A) UV-vis spectra of catechin (blue), PVA/CS nanofiber (black) and CA@PVA/CS nanofiber (red), (B) FTIR spectra of catechin (blue), PVA/CS nanofiber (red) and CA@PVA/CS nanofiber (black). (For interpretation of the references to colour in this figure legend, the reader is referred to the Web version of this article.)

biocompatibility, may be formed when these two are brought together. In terms of their molecular structure, PVA and chitosan are regarded to be "compatible polymers." The existence of hydrogen bonding sites in both polymers makes it possible for interactions between the functional groups, which is responsible for their compatibility. Films or coatings composed of PVA-chitosan blends have been utilized in a wide variety of applications. PVA and chitosan have advantages because they can create a film and are biocompatible; these properties make them great options for uses including wound dressings, drug delivery systems, and tissue engineering. The use of PVA-chitosan blends in controlled release systems has been investigated. Incorporating drugs or active substances into the blend provides regulated and targeted delivery by modulating and prolonging the release over time. It is important to keep in mind that the specific features and applications of PVA-chitosan blends can vary based on factors including the ratio of the two polymers, processing processes, and extra additives. Consequently, it is sometimes necessary to do additional study and optimization in order to customize their interactions for specific applications.

3.3. Drug loading capacity (%) and encapsulation efficiency (%)

Table 2 displays the observed DLC (%), and EE (%) for CA loaded CS/PVA nanofibers. The CA molecules loaded CS/PVA nanofibrous mats were found to significantly enhance either drug loading content (%) and encapsulation efficiency (%). Catechin encapsulated in chitosan nanofibers provides a variety of advantages. Catechin's stability is increased and its degradation has been stopped owing to the chitosan matrix. Catechin can be more effectively incorporated into a variety of environments attributable to the nanofiber structure's high surface area. Catechin-encapsulated chitosan nanofibers have a wide range of prospective applications. Catechin's antioxidant and antibacterial abilities make it useful for promoting wound healing and preventing infection in such applications. Catechin's long-lasting therapeutic benefits offer these nanofibers a promising candidate for use in drug delivery systems. They can also be used as additives in food packaging to prevent deterioration by microorganisms.

3.4. Antioxidant activity of CA@PVA/CS nanofiber

The antioxidant property of CA@PVA/CS nanofibers was evaluated by the DPPH method (Fig. 5A). DPPH assay was employed to measure the free radical scavenging capacities. The electron donor scaffolds that quench DPPH to DPPH-H are the best indicator for free radical scavenging. It is indicating that, the nanofiber scaffold containing catechin showed scavenging potency higher than ascorbic acid (* $p < 0.005$). Results revealed that CA@PVA/CS nanofiber exhibited antioxidant activity against DPPH at the lowest SC50 concentration (0.42 mg/ml) in scavenging (Fig. 5 B&C). The presence of chitosan and catechin shows a synergistic effect on the antioxidant mechanism and it can effectively stimulate enzymatic repair. CA@PVA/CS nanofiber is a promising candidate for diabetic

Table 2

The observed data for drug loading capacity (%) and encapsulation efficiency (%) of the prepared nanoformulations.

Formulations	DLC (%)	EE (%)
CA@CS/PVA	4.1 ± 0.50	75.16 ± 2.5

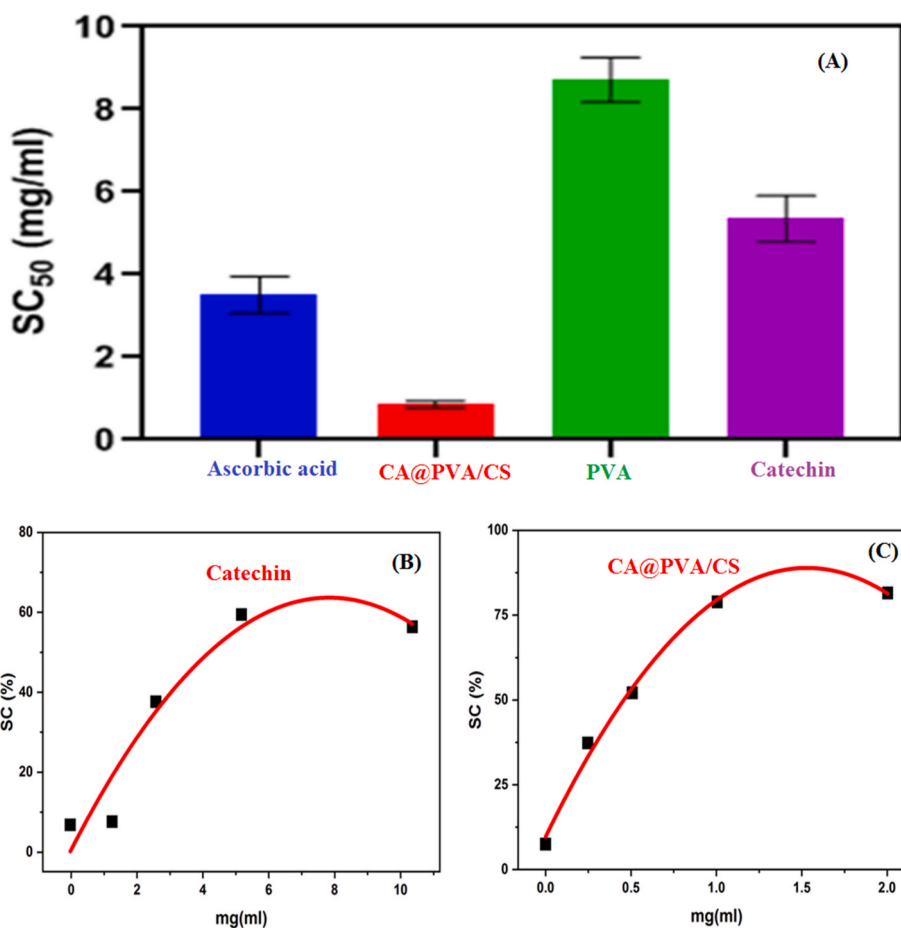


Fig. 5. Antioxidant activity of CA@PVA/CS nanofiber compare with Ascorbic acid and catechin (A), relative SC_{50} of prepared catechin and CA@PVA/CS nanofiber (B, C).

wound care applications.

3.5. Antibacterial activity of CA@PVA/CS nanofiber

The antibacterial potential of fabricated CA@PVA/CS nanofiber was assessed by well diffusion assay. The zone of bacterial inhibition was calculated in diameter after 24 h incubation period. The zone of inhibition at different concentrations of nanofiber treated bacterial were shown in Fig. 6. The nanofiber scaffolds have significant bactericidal properties compared to the selected commercial antibiotic ampicillin. The zone inhibition is an indicator of the antibacterial potential of CA@PVA/CS nanofibers. According to the zone of inhibition encapsulation catechin within PVA/CS nanofiber easily interact with gram-positive and gram-negative bacteria cells. As expected, the gram-positive bacterium is more sensitive to these mats. The negatively charged catechin attracted by a gram-positive bacteria cell wall and positively charged chitosan easily attracted by the gram-negative bacteria cell wall. The combination of catechin and chitosan leads to 78% of cell wall damage and ROS-mediated cell death in bacterial strains. A significant amount of inhibition zone was formed in all four bacteria (Fig. 7B) but compared to *E. coli* another three bacteria *S. aureus*, *S. epidermis*, and *P. aeruginous* are slightly higher. According to these antibacterial results, the fabricated CA@PVA/CS nanofiber scaffold is a highly suitable and efficient material for diabetic wound healing applications.

3.6. Biocompatibility of CA@PVA/CS nanofiber

Cytocompatibility of CA@PVA/CS nanofiber was assessed against L929 cells with two different methods including MTT assay and AO/EtBr dual staining. According to dual staining results, CA@PVA/CS nanofiber shows cell viability higher than 78% until 48 h post-exposure. Regarding MTT assay commercial anticancer drug cisplatin shows only 32% of viable cells at the highest concentration of 100 μ g/ml. Alone catechin-treated cells show 70% of cell viability (Fig. 7A). The combination of catechin and PVA/CS nanofibers enhanced the biocompatibility of fibroblast L929 cells. In contrast, a nanofiber scaffold provides more advantages to nutrient transport into cells. Microscopic images of CA@PVA/CS nanofiber treated cells show a higher level of green fluorescence, which indicates

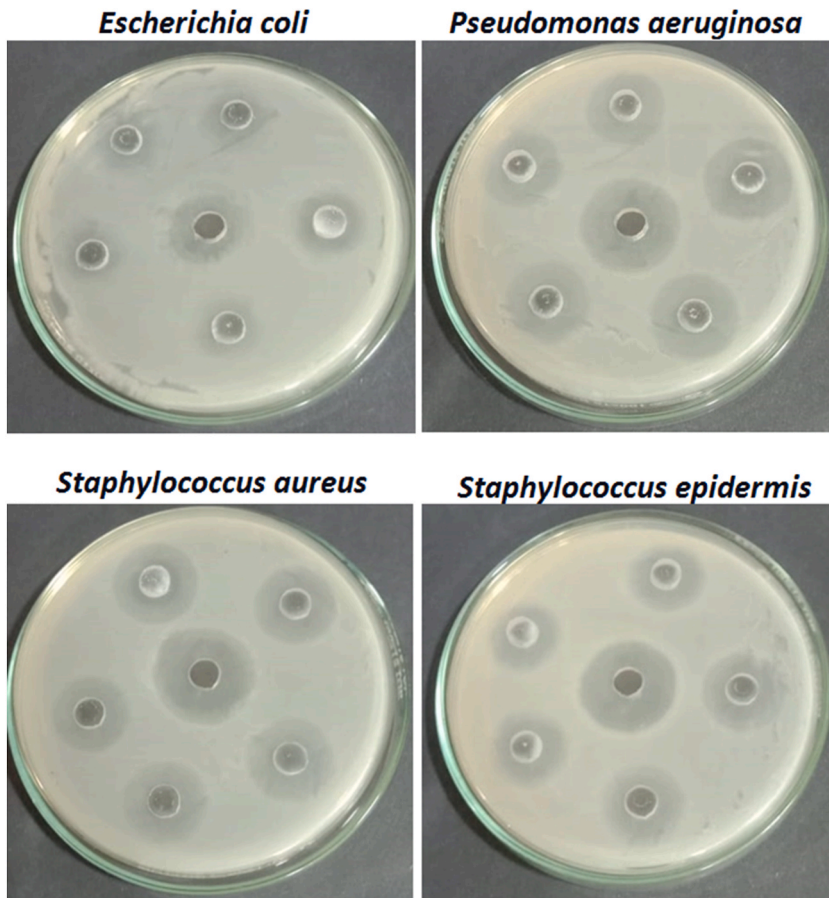


Fig. 6. Antibacterial potential of CA@PVA/CS nanofiber at different concentrations (20–100 µg/ml).

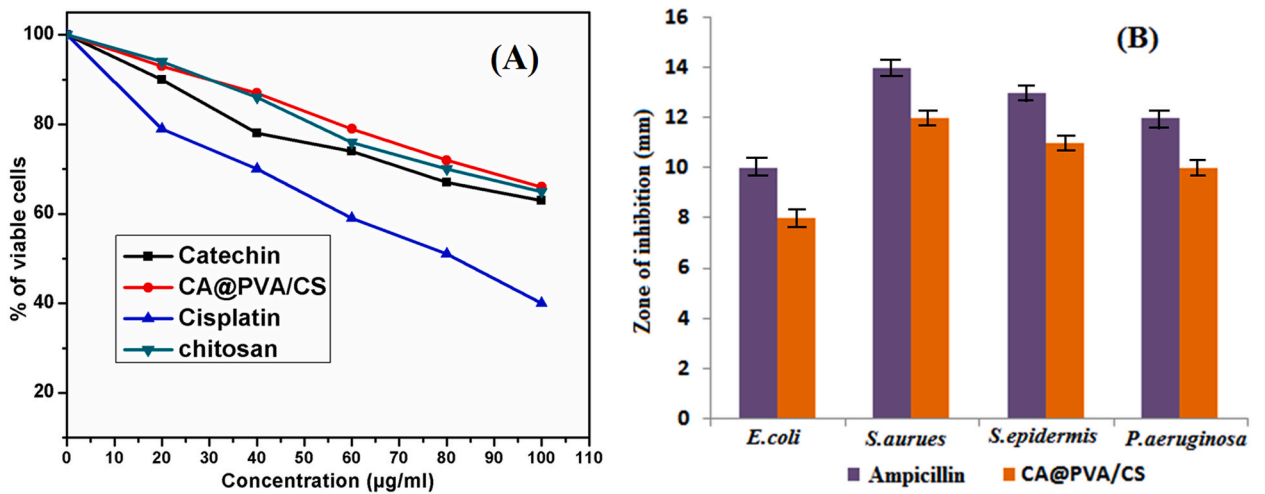


Fig. 7. (A) Cytotoxicity of CA@PVA/CS nanofiber compare with commercial anticancer drug Ampicillin and (B) Bacterial zone of inhibition at highest concentration (100 µg/ml) against wound infected bacteria.

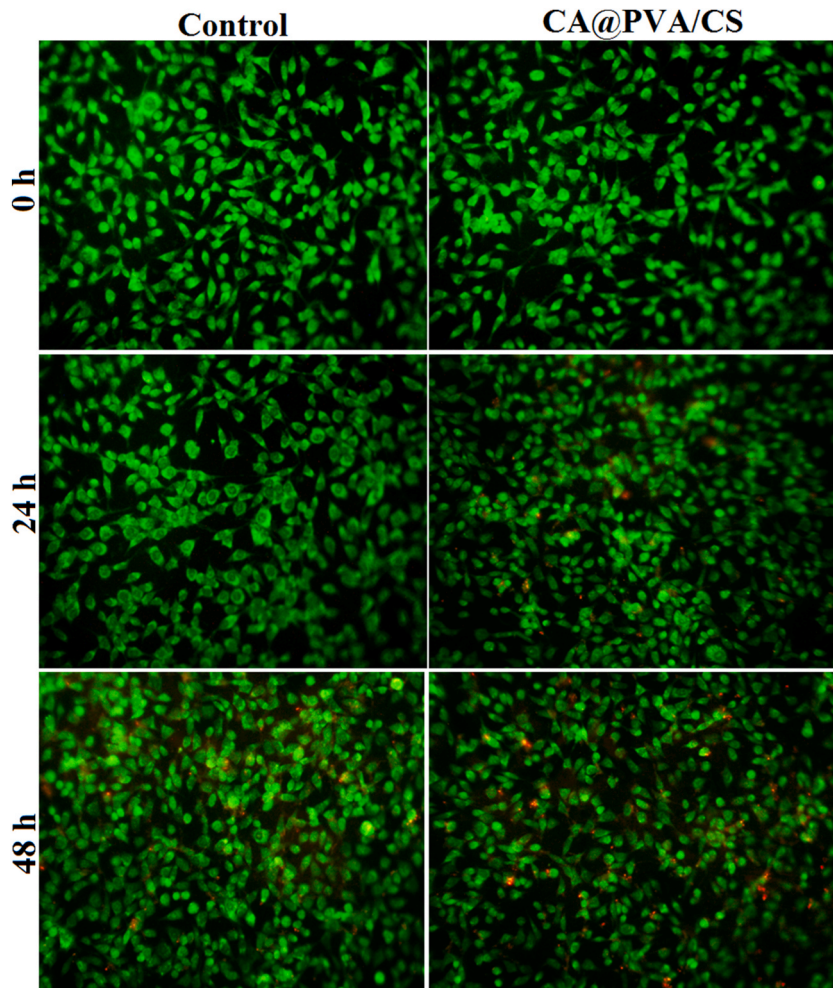


Fig. 8. Fluorescence microscopic images of CA@PVA/CS nanofiber treated cells in AO/EtBr dual staining after post exposure at different time intervals (0, 24 and 48 h) at 20x magnification.

healthy live cells after 48 h of treatment (Fig. 8). The present study concluded that the CA@PVA/CS nanofiber is a more biocompatible and suitable material for diabetic wound healing applications.

3.7. The wound healing potential of CA@PVA/CS nanofiber

The wound healing property of the fabricated nanofiber scaffold was assessed by *in vitro* wound scratch assay against L929 cell lines. The results exhibit that the CA@PVA/CS nanofibers regulate the regeneration of fibroblast cells and initiate the healing mechanism of scratched cells. The wound healing potential of materials has been determined by fibroblast accumulation and collagen deposition in specific wound sites. We found excellent cell migration and regeneration after 12 h of pipette scratch as shown in Fig. 9. Releasing of the catechin molecule stimulates the protein secretion and leads cellular migration process. Dual polymeric nanofiber scaffolds can promote a faster wound healing process and biocompatibility of the material. The inverted phase contrast microscopic images showed that a remarkable increase in cell regeneration potential, compared to control groups is fourfold higher. The CA@PVA/CS nanofiber exposes the progressive epithelization without external inflammation, in all treated groups. According to Fig. 9, the percentage of wound healing increases with the time increase of post-exposure to nanofiber, especially after 48 h of complete wound closure has been achieved. The overall *in vitro* wound scratch assay confirmed that, the CA@PVA/CS nanofiber more suitable and efficient material for the diabetic wound care [56–60].

4. Discussion

Diabetic ulcer-related wound infections have a dangerous effect on public health it can lead to death. Diabetic wounds are very different from normal wounds and so easy to bacterial infections due to the oxidative stress of surrounding wound tissues. Electrospun

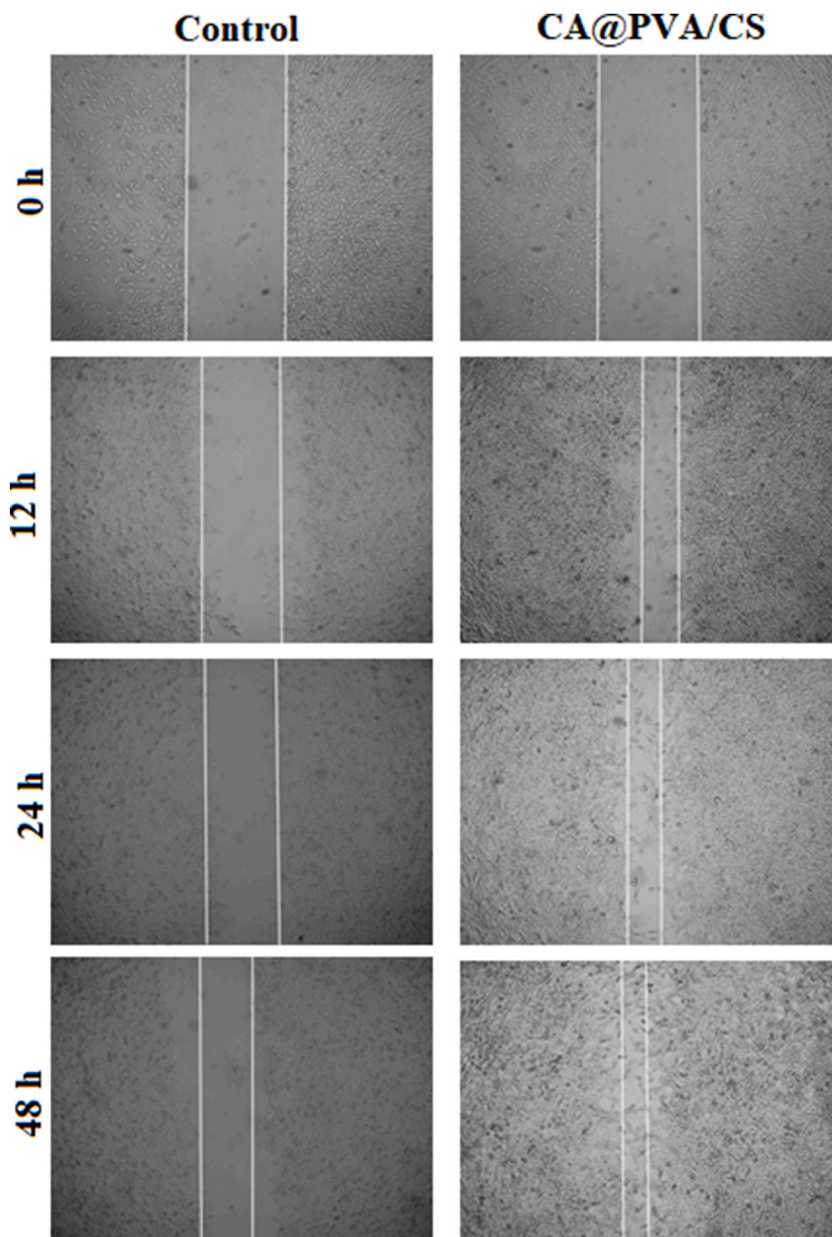


Fig. 9. Inverted phase contrast microscopic images of CA@PVA/CS nanofiber treated L929 cells post *in vitro* wound scratch assay at different time intervals (0, 12, 24, and 48 h) at 20x magnification.

nanofibers has great consideration in the designing of wound dressings in the past four decades [61,62]. There are lots of biopolymers employed for electrospinning, techniques, chitosan is the most valuable biopolymer for the design of electrospun fibers, due to its biocompatible, nontoxic, anti-microbial, as well as biodegradable properties. The blended electrospun nanofibers possess enhanced stability, mechanical property, and biocompatibility, which are essential for wound healing [63,64]. Skin damage causes a higher level of ROS production in wound sites, lead protein, nucleic acid damage, and cell death [65,66]. It has been determined that CS may promote cell proliferation *in vivo* in a strange manner. Furthermore, after CS was administered, both polymorphonuclear (PMN) and mononuclear (MN) cells started to migrate immediately. In order to promote cell mobility, PMN and MN break down CS into its low molecular weight oligomers and monomers. In this work, the overall results revealed that catechin-encapsulated PVA/CS nanofiber exhibits considerable antibacterial and antioxidant ability with synergic effects in wound healing. The enhanced antibacterial activity of the CA@PVA/CS nanofiber combination showed attractive improvement in the overall wound healing process. It brings out an efficient antibiotic with combinations of antibacterial and antioxidant potentials. In the antibacterial experiments, CA@PVA/CS nanofiber scaffolds are highly sensitive to gram-positive and gram-negative wound pathogens. Investigation of biocompatibility

studies concluded no cytotoxic effects against human fibroblast cells, while cell viability of fiber-treated cells significantly increased over a long period. It indicates that nanofiber had no toxic effect *in vitro* conditions [67]. Also, a promising antibiotic for wounded cell regeneration. Finally, overall cell line, antioxidant assay, and antibacterial studies concluded that the CA@PVA/CS nanofibers scaffolds could be a suitable material for diabetic wound care and will facilitate effective diabetic wound healing, addition it can reduce the cost of treatment. CA@PVA/CS nanofibers exert their beneficial activity on wound closure whereas the incorporation of catechin enhances wound closure within a short period. The most plausible mechanism could be due to the control of ROS generation by catechin. The elimination of skin cell ROS can serve as a stimulant of cell proliferation leading to wound-healing effects. Antibacterial efficacy conferred by catechin in chitosan/PVA nanofibers might have promoted the rate of wound healing. The porous-natured nanofiber scaffolds conferring better moisture absorption and sufficient oxygen supply might be another reason for fast wound contraction. The wound healing potential of the CA@PVA/CS nanofibers membranes enabled it to be used as a dressing material for diabetic wound healing. Many research reports are stating the importance of PVA/chitosan nanofibers in enhancing the wound healing process. For instance, the effect of catechin-encapsulated PVA/chitosan scaffolds on antibacterial and wound healing efficacy was determined by enhanced wound contraction. The nano formulation-based fabrication of CA@PVA/CS scaffolds might be an ideal material for diabetic wound healing applications [68,69].

5. Conclusion

The CA@PVA/CS nanofibers were designed and fabricated by using the electrospinning method. The nanofibers showed reliable antibacterial, anti-oxidant potential and very encouraging results in the wound healing process. The nanofiber scaffolds exhibited outstanding antibacterial efficacy against skin infectious bacteria. CS@PVA/CS nanofiber also manifested higher antioxidant activity which makes them promising material for diabetic wound healing. The present study demonstrated that that the CA@PVA/CS nanofibers can serve as useful dressing materials in diabetic wounds when compared to the control nanofibrous mat without CA encapsulation. In the future, the exact healing mechanism of faster wound healing of CA@PVA/CS nanofibers scaffolds can be explored by animal models.

Funding

This study was supported by Scientific Project of Changsha First Hospital (No. Y2021-30), Research Project of Hunan Provincial Health Commission (No. 202103060456), and Hunan Province Clinical Medical Technology Innovation Guidance Project (No. 2021SK53111).

Data Availability Statement

The data that support the findings of this study are available from the corresponding author, upon reasonable request.

CRediT authorship contribution statement

Yunting Hu: Resources, Investigation, Formal analysis. **Li Hu:** Resources, Investigation, Formal analysis. **Li Zhang:** Writing – original draft, Methodology, Data curation. **Juan Chen:** Writing – original draft, Methodology, Data curation. **Huiyu Xiao:** Methodology, Investigation, Data curation. **Bin Yu:** Validation, Software. **Yinzhen Pi:** Writing – review & editing, Validation, Supervision, Project administration.

Declaration of competing interest

The authors declare that they have no known competing financial interests or personal relationships that could have appeared to influence the work reported in this paper.

References

- [1] G. Frykberg Robert, Challenges in the treatment of chronic wounds, *Adv. Wound Care* (2015).
- [2] S. Suarez Easton, N. Zafran, G. Garmi, R. Salim, Post cesarean wound infection prevalence, impact, prevention and management challenges, *Int. J. women health* 9 (2017) 81.
- [3] B. Delmore, J.M. Cohen, D. Oneill, A. Chu, V. Pham, E. Chiu, Reducing postsurgical wound complications a critical review, *Adv. Skin Wound Care* 30 (2017) 272–285.
- [4] T. An, Y. Chen, Y. Tu, P. Lin, Mesenchymal stromal cell derived extracellular vesicles in the treatment of diabetic foot ulcers: application and challenges, *Stem cell. Rev. Rep.* 17 (2) (2021) 369–378.
- [5] L.R. Kalan, M.B. Brennan, The role of the microbiome in nonhealing diabetic wounds, *Ann. N.Y. Acad. Sci* 1435 (1) (2019) 79–92.
- [6] S. Priyadarisini, A. Whelchel, S. Nicholas, R. Sharif, K. Riaz, D. Karamichos, Diabetic keratopathy insights and challenges, *Surv. Ophthalmol.* 65 (5) (2020) 513–529.
- [7] L.M. Jones, C. Rubadue, N.V. Brown, S. Khandelwal, R.A. Coffey, Evaluation of TCOM/HBOT practice guideline for the treatment of foot burns occurring in diabetic patients, *Burns* 41 (3) (2015) 536–541.
- [8] G.C. Gurtner, S. Werner, Y. Barrandon, M.T. Longaker, Wound repair and regeneration, *Nature* 453 (2008) 314–321.
- [9] R. Augustine, N. Kalarikkal, S. Thomas, Advancement of wound care from grafts to bioengineered smart skin substitutes, *Prog. Biomat.* 3 (2–4) (2014) 103–113.

- [10] N. Zoller, E. Valesky, M. Butting, M. Hofmann, S. Kippenberger, J. Bereiter-Hahn, A. Bernd, R. Kaufmann, Clinical application of a tissue-cultured skin autograft an alternative for the treatment of nonhealing or slowly healing wounds, *Dermatology* 229 (3) (2014) 190–198.
- [11] H. Savoiji, B. Godau, M.S. Hassani, M. Akbari, Skin tissue substitutes and biomaterial risk assessment and testing, *Front. Bioeng. Biotechnol.* 6 (2018) 86.
- [12] M. Abbas, T. Hussain, M. Arshad, A.R. Ansari, A. Irshad, J. Nisar, F. Hussain, N. Masood, A. Nazir, M. Iqbal, Wound healing potential of curcumin cross-linked chitosan/polyvinyl alcohol, *Int. J. Biol. Macromol.* 140 (2019) 871–876.
- [13] S. Tejada, A. Manayi, M. Daglia, S.F. Nabavi, A. Sureda, Z. Hajheydari, O. Gortzi, H. Pazoki-Toroudi, S.M. Nabavi, Wound healing effects of curcumin a short review, *Curr. Pharm. Biotechnol.* 17 (11) (2016) 1002–1007.
- [14] A. Gaspar-Pintilieșcu, A.M. Stanciuc, O. Craciunescu, Natural composite dressings based on collagen, gelatin and plant bioactive compounds for wound healing: a review, *Inter. J. Biol. Macromolec.* 138 (2019) 854–865.
- [15] D. Gopinath, M.R. Ahmed, K. Gomathi, K. Chitra, P. Sehgal, P. Jayakumar, Dermal wound healing processes with curcumin incorporated collagen films, *Biomaterials* 25 (10) (2004) 1911–1917.
- [16] M. Rezaei, S. Oryan, M.R. Nourani, M. Mofid, M. Mozafari, Curcumin nanoparticle incorporated collagen/chitosan scaffolds for enhanced wound healing, *Bioinspired, Biomimetic Nanobiomater.* 7 (3) (2018) 159–166.
- [17] T. Nakanishi, K. Mukai, H. Yumoto, K. Hirao, Y. Hosokawa, T. Matsuo, Anti-inflammatory effect of catechin on cultured human dental pulp cells affected by bacteria-derived factors, *Eur. J. Oral Sci.* 118 (2010) 145–150.
- [18] N. Lu, P. Chen, Q. Yang, Y.Y. Peng, Anti- and pro-oxidant effects of (+)-catechin on hemoglobin-induced protein oxidative damage, *Toxicol. Vitro* 25 (4) (2011) 833–838.
- [19] Y. Jiang, Z. Jiang, L. Ma, Q. Huang, Advances in Nanodelivery of green tea catechins to enhance the anticancer activity, *Molecules* 26 (2021) 3301.
- [20] N.C. Gordon, D.M. Wareham, Antimicrobial activity of the green tea polyphenol -epigallocatechin-3-gallate (EGCG) against clinical isolates of *Stenotrophomonas maltophilia*, *Int. J. Antimicrob. Agents* 36 (2010) 129–131.
- [21] Y.M. Huang, Q.Q. Zhu, X.Y. Yang, H.H. Xu, et al., Wound healing can be improved by epigallocatechin gallate through targeting Notch in streptozotocin induced diabetic mice, *FASEB J* 33 (2019) 953–964.
- [22] S. Trompezinski, A. Denis, D. Schmitt, J. Viac, Comparative effects of polyphenols from green tea (EGCG) and soybean (genistein) on VEGF and IL-8 release from normal human keratinocytes stimulated with the proinflammatory cytokine TNF alpha, *Arch. Dermatol. Res.* 295 (2003) 112–116.
- [23] S.R. Avila, G.P.D. Schuenck, et al., High antibacterial in vitro performance of gold nanoparticles synthesized by epigallocatechin 3-gallate, *J. Mater. Res.* 36 (2021) 518–532.
- [24] Y.R. Wu, H.J. Choi, Y.G. Kang, J.K. Kim, J.W. Shin, In vitro study on anti-inflammatory effects of epigallocatechin-3-gallateloading nano and microscale particles, *Int. J. Nanomed.* 12 (2017) 7007–7013.
- [25] F. Pires, J.K. Santos, D. Bitoque, G.A. Silva, A. Marletta, V.A. Nunes, P.A. Ribeiro, J.C. Silva, M. Raposo, Polycaprolactone/gelatin nanofiber membranes containing EGCG-loaded liposomes and their potential use for skin regeneration, *ACS Appl. Bio Mater.* 2 (2019) 4790–4800.
- [26] Y.W. Wang, C.C. Liu, J.H. Cherng, C.S. Lin, S.J. Chang, Z.J. Hong, C.C. Liu, et al., Biological effects of chitosan based dressing on hemostasis mechanism, *Polymers* 11 (11) (2019) 1906.
- [27] J.R. Pragłowska, M. Piatkowski, V. Deineka, L. Janus, V. Kornienko, E. Husak, et al., Chitosan based bioactive hemostatic agents with antibacterial properties synthesis and characterization, *Molecules* 24 (14) (2019) 2629.
- [28] P. Ramasamy, A. Shanmugam, Characterization and wound healing property of collagen-chitosan film from *Sepia kobeiensis* (Hoyle, 1885), *Int. J. Biol. Macromol.* 74 (2015) 93–102.
- [29] N. Amiri, S. Ajami, A. Shahroodi, N. Jannatabadi, S. Amiri Darban, B.S. Fazly Bazzaz, E. Pishavar, F. Kalalinia, J. Movaffagh, Teicoplanin loaded chitosan PEO nanofibers for local antibiotic delivery and wound healing, *Int. J. Biol. Macromol.* 162 (2020) 645.
- [30] S. Bayat, N. Amiri, E. Pishavar, F. Kalalinia, J. Movaffagh, M. Hashemi, Bromelain loaded chitosan nanofibers prepared by electrospinning method for burn wound healing in animal models, *Life Sci.* 229 (2019) 57–66.
- [31] Z. Chen, P. Wang, B. Wei, X. Mo, F. Cui, Electrospun collagen chitosan nanofiber a biomimetic extracellular matrix for endothelial cell and smooth muscle cell, *Acta Biomater.* 6 (2) (2010) 372–382.
- [32] T.T. Yuan, P.M. Jenkins, A.M. DiGeorge Foushee, A.R. Jockheck Clark, J.M. Stahl, Electrospun chitosan/polyethylene oxide nanofibrous scaffolds with potential antibacterial wound dressing applications, *J. Nanomater.* (2016) 6231040.
- [33] M. Ignatova, I. Rashkov, N. Manolova, Drug-loaded electrospun materials in wound-dressing applications and in local cancer treatment, *Expert Opin. Drug Deliv.* 10 (4) (2013) 469–483.
- [34] P.C. Berscht, B. Nies, A. Liebendorfer, J. Kreuter, In vitro evaluation of biocompatibility of different wound dressing materials, *J. Mater. Sci. Mater. Medicine.* 6 (4) (1995) 201–205.
- [35] R.H. Rubin, Surgical wound infection epidemiology, pathogenesis, diagnosis and management, *BMC Infect. Dis.* 6 (1) (2006) 1–2.
- [36] S. Saghazadeh, C. Rinoldi, M. Schot, et al., Drug delivery systems and materials for wound healing applications, *Adv. Drug Deliv. Rev.* 127 (2018) 138–166.
- [37] N.K. Rajendran, S.S.D. Kumar, N.N. Hourelid, H. Abrahamse, A review on nanoparticle-based treatment for wound healing, *J. Drug Deliv. Sci. Technol.* 44 (2018) 421–430.
- [38] M. Kasithevar, P. Periakaruppan, S. Muthupandian, M. Mohan, Antibacterial efficacy of silver nanoparticles against multi drug resistant clinical isolates from post-surgical wound infections, *Microb. Pathog.* 107 (2017) 327–334.
- [39] S. Rathinavel, S. Ekambaram, P.S. Korrapati, D. Sangeetha, Design and fabrication of electro spun SBA-15-incorporated PVA with curcumin a biomimetic nano scaffold for skin tissue engineering, *Biomed. Mat.* 15 (3) (2020) 035009.
- [40] M. Gizaw, J. Thompson, A. Faglie, S.Y. Lee, P. Neuenschwander, S.F. Chou, Electro spun fibers as a dressing material for drug and biological agent delivery in wound healing applications, *Bioengineering* 5 (1) (2018) 9.
- [41] M.A. Hasan Kohal, L. Tayebi, M. Ghorbani, Curcumin loaded naturally based nanofibers as active wound dressing mats morphology, drug release, cell proliferation and cell adhesion studies, *New J. Chem.* 44 (2020) 10343.
- [42] S.B. Qasim, M.S. Zafar, S. Najeeb, Z. Khurshid, A.H. Shah, S. Husain, I.U. Rehman, Electrospinning of chitosan-based solutions for tissue engineering and regenerative medicine, *Int. J. Mol. Sci.* 19 (2) (2018) 407.
- [43] C. Gao, L. Zhang, J. Wang, M. Jin, Q. Tang, et al., Electrospun nanofibers promotes wound healing theories, techniques, and perspectives, *J. Mater. Chem. B* 9 (14) (2021) 3106–3130.
- [44] Y.J. Chu, D.M. Yu, P.H. Wang, J. Xu, D.Q. Li, M. Ding, Nanotechnology promotes the full-thickness diabetic wound healing effect of recombinant human epidermal growth factor in diabetic rats, *Wound Repair Regen.* 18 (2010) 499–505.
- [45] R. Ahmed, M. Tariq, I. Ali, et al., Novel electro spun chitosan/polyvinyl alcohol/zinc oxide nanofibrous mats with antibacterial and antioxidant properties for diabetic wound healing, *Int. J. Biol. Macromol.* 120 (2018) 385–393.
- [46] D.A. Locilento, L.A. Mercante, R.S. Andre, et al., Biocompatible and biodegradable electrospun nanofibrous membranes loaded with grape seed extract for wound dressing application, *J. Nanomater.* (2019) 2472964.
- [47] R. Prabhu, N. Sughanthi, Anticancer, antibiofilm and antimicrobial activity of fucoic acid loaded zeolitic imidazole framework fabricated by one -pot synthesis method, *Appl. Nanosci.* (2021) 1–19.
- [48] A.S. Alvarez Suarez, S.G. Dastager, N. Bogdanchikova, et al., Electrospun fibers and sorbents as a possible basis for effective composite wound dressings, *Micromachines* 11 (4) (2020) 441.
- [49] L. Guadagno, M. Raimondo, L. Vertuccio, E.P. Lamparelli, M.C. Ciardulli, P. Longo, A. Mariconda, G. Della Porta, R. Longo, Electrospun membranes designed for Burst release of new gold-Complexes inducing Apoptosis of Melanoma cells, *Int. J. Mol. Sci.* 23 (2022) 7147.
- [50] M.V. Natu, H.C. de Sousa, M.H. Gil, Effects of drug solubility, state and loading on controlled release in bicomponent electrospun fibers, *Int. J. Pharm.* 397 (2010) 50–58.

- [51] Guadagno, et al., Electrospun membranes designed for Burst release of new gold-Complexes inducing Apoptosis of Melanoma cells, *Int. J. Mol. Sci.* 23 (13) (2022) 7147.
- [52] W. Cui, X. Li, S. Zhou, J. Weng, Investigation on process parameters of electrospinning system through Orthogonal experimental design, *J. Appl. Polym. Sci.* 103 (2007) 3105–3112.
- [53] T.T. Lia, M. Yana, Y. Zhonga, H.T. Rena, C.W. Louc, S.Y. Huang, J.H. Lin, Processing and characterizations of rotary linear needleless electrospun polyvinyl alcohol (PVA)/Chitosan(CS)/Graphene(Gr) nanofibrous membranes, *J. Mater. Res. Technol.* 8 (6) (2019) 5124–5132.
- [54] Z. Czibulya, A. Csik, C. Hegedüs, et al., The effect of the PVA/Chitosan/Citric acid ratio on the hydrophilicity of electrospun nanofiber Meshes, *Polymers* 13 (2021) 3557.
- [55] U.S. Sajeev, K.A. Anand, D. Menon, Control of nanostructures in PVA, PVA/chitosan blends and PCL through electrospinning, *Bull. Mater. Sci.* 31 (2008) 343–351.
- [56] W.A. Sarhan, H.M. Azzazy, I.M. El-Sherbiny, Honey/chitosan nanofiber wound dressing enriched with *Allium sativum* and *Cleome droserifolia*: enhanced antimicrobial and wound healing activity, *ACS Appl. Mater. Interfaces* 9 (37) (2017) 31617–31627.
- [57] K. Azuma, R. Izumi, Osaki, S. Ifuku, M. Morimoto, H. Saimoto, O. Takashima, Chitin, chitosan, and its derivatives for wound healing: old and new materials, *J. Funct. Biomater.* 9 (3) (2018) 42.
- [58] R. Jayakumar, D. Menon, K. Manzoor, Preparation and evaluation of chitosan–gelatin/nano bioglass ceramic composite scaffolds for tissue engineering, *Carbohydrate Polymers* 82 (2) (2010) 472–479.
- [59] L. Satish, G. Rajalakshmi, Chitosan nanofiber sheets with enhanced wound-healing properties for skin tissue engineering applications, *J. Appl. Polym. Sci.* 136 (16) (2019) 47394.
- [60] P.T. Sudheesh Kumar, V.K. Lakshmanan, T.V. Anilkumar, C. Ramya, P. Reshmi, Preparation and characterization of novel α -cyano-4-hydroxycinnamic acid/chitosan composite nanofibers for wound dressing applications, *Int. J. Biol. Macromol.* 50 (2012) 44–48.
- [61] K.P. Akshay Kumar, E.N. Zare, R. Torres Mendieta, et al., Electrospun fibers based on botanical, seaweed, microbial, and animal sourced bio-macromolecules and their multidimensional applications, *Int. J. Biol. Macromol.* 171 (2021) 130–149.
- [62] Y. He, Y. Jin, X. Wang, et al., An antimicrobial peptide-loaded gelatin/chitosan nanofibrous membrane fabricated by sequential layer by layer electrospinning and electro spraying techniques, *Nanomaterials* 8 (5) (2018) 327.
- [63] A.C. Alavarse, F.W. De Oliveira Silva, J.T. Colque, V.M. Da Silva, T. Prieto, E.C. Venancio, J.J. Bonvent, Tetracycline hydrochloride-loaded electro spun nanofibers mats based on PVA and chitosan for wound dressing, *Mat. Sci. Eng. C* 77 (2017) 271–281.
- [64] P.G. Rodriguez, F.N. Felix, D.T. Woodley, E.K. Shim, The role of oxygen in wound healing: a review of the literature, *Dermatol. Surg.* 34 (9) (2008) 1159–1169.
- [65] J.D. Malcor, F.M. Gerin, Biomaterial functionalization with triple-helical peptides for tissue engineering, *Acta Biomater.* 148 (2022) 1–21.
- [66] G. Liu, Y. Zhou, Z. Xu, Z. Bao, L. Zheng, J. Wu, Janus hydrogel with dual antibacterial and angiogenesis functions for enhanced diabetic wound healing, *Chinese Chem Let* 34 (4) (2023) 107705.
- [67] X. Gao, S. Han, R. Zhang, G. Liu, J. Wu, Progress in electro spun composite nanofibers: composition, performance and applications for tissue engineering, *J. Mater. Chem. B* 7 (45) (2019) 7075–7089.
- [68] H. Wu, J. Fan, C.C. Chu, J. Wu, Electrospinning of small diameter 3-D nanofibrous tubular scaffolds with controllable nanofiber orientations for vascular grafts, *J. Mat Sci: Mater Med* 21 (12) (2010) 3207–3215.
- [69] H. Zhong, J. Huang, J. Wu, J. Du, Electrospinning nanofibers to 1D, 2D, and 3D scaffolds and their biomedical applications, *Nano Res.* 15 (2) (2022) 787–804.